

Anomalous Thermomechanical Behaviour of Carbon Nanotube Bundle

S.V. Dmitriev^{1,2}, L.Kh. Galiakhmetova¹ and E.A. Korznikova^{1,2}

¹Institute for Metals Superplasticity Problems, Russian Academy of Sciences, Khalturina 39, Ufa 450001, Russia

²Institute of Molecule and Crystal Physics, Ufa Research Center of Russian Academy of Sciences, Prospekt Oktyabrya 151, Ufa 450075, Russia

Received: August 09, 2021

Abstract. The molecular dynamics method is used to calculate the dependence of pressure on temperature at a constant volume for a bundle of carbon nanotubes (CNTs) considered under plane strain conditions. A chain model with a significantly reduced number of degrees of freedom is used for modeling. The influence of the CNT diameter is analyzed. It was found that for some parameters of the model, the pressure in the CNT bundle can decrease with increasing temperature, which is equivalent to the effect of negative thermal expansion.

1. INTRODUCTION

Most materials have a positive coefficient of thermal expansion (CTE), increasing in size when heated. CTE is one of the fundamental characteristics of materials, very important for engineering practice. CTE is positive due to the asymmetry of interatomic potentials, which is true for any type of chemical bond. The appearance of negative thermal expansion (NTE) means that there are some features in the structure of the material that compensate for the influence of the asymmetry of interatomic potentials. In some complex systems, NTE arises from lateral vibrations of the materials [1] or from low-frequency rigid-unit modes [2]. The CTE of metal nanowires can be reduced due to elastic softening of materials, as well as due to surface stress [3]. A decrease in the CTE can lead to NTE if the Young's modulus of the nanowire is sufficiently lowered, while the surface stress of the nanowire remains sufficiently high [3].

In the review article [4] a number of different cases leading to NTE are identified, some of which are associated with rotation of rigid polyhedral groups of atoms, and in others transverse acoustic modes play an important role.

With the use of molecular dynamics simulations it was shown that graphene origami structures provide tunable coefficients of thermal expansion from large negative to large positive [5]. The NTE behavior can emerge as a size-reduction effect caused by the intrinsic nanoparticles surface pressure at the nanoscale [6].

Thermal expansion of Ni nanowires electrodeposited into self-organized nanoporous amorphous aluminum oxide membranes without an Al substrate has been measured using X-ray diffraction between 110 K and 350 K [7]. An average thermal expansion of the Ni nanowires along the wire axis was found to be $-(1.6 \pm 1.5) \times 10^{-6} \text{ K}^{-1}$.

A very low coefficient of thermal expansion can be achieved in shape memory NiTi alloy over a wide temperature span along a certain direction [8]. NTE has been found in a number of ferromagnetic and ferrimagnetic materials and recently even in antiferromagnetic materials [9]. It has been found that the $\text{ScCo}(\text{CN})_6$ of Prussian blue analogues has a large isotropic negative thermal expansion in a wide temperature range from 25 K to 600 K [10]. A real-space model of atomic motion in the prototypical NTE material scandium trifluoride, ScF_3 , has been developed from total neutron scattering data [11] and it

Corresponding author: S.V. Dmitriev, e-mail: dmitriev.sergey.v@gmail.com

has been shown that NTE in this material depends not only on rigid unit modes of scandium octahedral, but also on modes that distort these octahedra. A new concept of “average atomic volume” has been proposed to find new NTE open-framework materials [12] and two NTE compounds, $\text{AgB}(\text{CN})_4$ and $\text{CuB}(\text{CN})_4$, have been discovered. Many anomalies of the properties of water at low temperatures and negative pressures or nitrogen at megabar pressures and high temperatures are related to zero and negative CTE [13].

A symmetry-motivated approach to analyzing X-ray pair distribution functions has been used to study the mechanism of NTE in ScF_3 and CaZrF_6 [14]. It has been found that the flexibility of M-F-M linkages (M = Ca, Zr, Sc) due to dynamic rigid scissoring modes facilitates the observed NTE behavior.

The tolerance factor of the Ruddlesden-Popper oxide Ca_2MnO_4 can be tuned by isovalent substitutions, leading to the uniaxial coefficient of linear thermal expansion changing through large negative to positive values [15]. NTE has been found in some magnetic functional materials due to the magnetovolume effect [16]. Scandium fluoride (ScF_3) is an NTE material showing a strong lattice contraction up to 1000 K and expanding at higher temperatures. The NTE effect in ScF_3 has been analyzed in the temperature range from 300 K to 1600 K using *ab initio* molecular dynamics [17]. It has been shown that the origin of the NTE in ScF_3 is due to the interplay between expansion and rotation of ScF_6 octahedra [17]. Anharmonic free-energy calculations based on density functional theory have been performed to demonstrate that the quasiharmonic approximation breaks down for ScF_3 and the quartic anharmonicity is essential to reproduce the observed transition from negative to positive thermal expansion [18].

Various strategies for systematically tuning the CTE in a diverse series of metal–organic frameworks (MOFs) have been demonstrated [19]. NTE is a common phenomenon in MOFs and the introduction of additional linkages in a parent framework has been shown to be an effective approach to alter the NTE behavior in MOFs [20].

In the work [21] the two main mechanisms for isotropic NTE were summarized, a combined metric of NTE capacity was proposed, and known NTE materials were classified according to the proposed metrics (magnitude and range of NTE effect).

Inelastic neutron scattering measurements have been performed at different temperatures on a powdered sample of $\text{ZnNi}(\text{CN})_4$ to probe phonon dynamics and explain the NTE behavior of this material [22]. In the work [23] it has been proposed that the lattice parameter is a key element for controlling thermal expansion of a mate-

rial. The lattice parameter can be controlled through external pressure, chemical or other methods. The single-well potential energy of the polyhedra rotations (or atomic transverse vibrations) can be turned into a quartic anharmonic potential or into a double-well potential. In the former case the NTE is enhanced, while in the latter case it is suppressed [23].

A model of a material consisting of interconnected array of ring and sliding rod structures made from conventional materials has been developed to model NTE, negative moisture expansion, and negative compressibility [24].

A new NTE compound has been found in the work [25], $\text{FeFe}(\text{CN})_6$ Prussian blue analogue, where the average linear coefficient of thermal expansion is $-4.26 \times 10^{-6} \text{ K}^{-1}$ in the range of temperature from 100 to 450 K. Using different experimental techniques it has been shown that the transverse thermal vibrations of C and N atoms are crucial for the occurrence of the NTE of Prussian blue analogues [25].

In this work, we consider a bundle of carbon nanotubes (CNTs) under plane strain conditions. This material has unusual mechanical properties, since it consists of highly deformable structural elements [26-31]. The role of such elements is played by the cross-sections of CNTs, which can collapse under pressure or perform bending vibrations excited by heating. In particular, we look at the NTE effect in this material.

2. MODEL

In this work, bundle of zigzag, single walled CNTs of the same diameter is considered under plane strain conditions, which means that the axial deformation of CNTs is equal to zero and the problem becomes two-dimensional. CNT cross sections create in the x,y plane a densely packed structure, as shown in Fig. 1. Periodic boundary conditions are applied in two directions. Computational cell contains 12 vertical rows of CNTs with 10 CNTs in each row. Total number of CNTs is 120.

Let $\rho = 1.418 \text{ \AA}$ is the interatomic distance in the CNT wall. Then the distance between the nearest carbon atoms, in projection onto the x,y plane, will be equal to $a = \rho^{3/2}/2$. CNT cross section is presented by an even number of carbon atoms N . Each atom is a member of a rigid atomic chain normal to the x,y plane. CNT diameter is $D = a/\sin(\pi/N)$. For N much greater than p , $D = aN/p$. The equilibrium distance between the walls of neighboring CNTs, d , is found as a result of structure relaxation at zero temperature. The distance between the centers of neighboring CNTs is $A = D + d$.

In order to study the effect of CNT diameter, we consider the bundles of CNTs with $N=20, 30, 40, 50, 60$, and 70. In Fig. 1, a part of the computational cell is shown

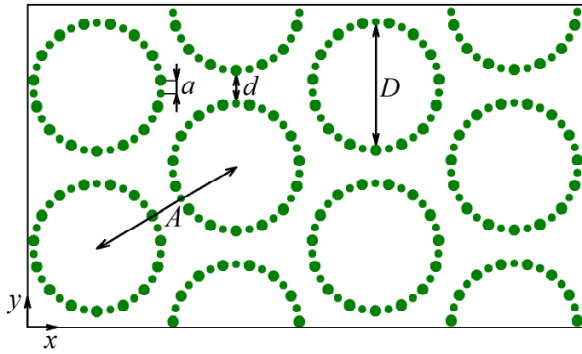


Fig. 1. Geometry of the CNT bundle under plain strain conditions. CNTs have zigzag chirality $(m,0)$. CNT cross sections create a close packed molecular crystal. Each carbon atom represents a rigid chain of atoms normal to the x,y plane. Atoms moving on the x,y plane have two degrees of freedom. Two sets of chains shifted with respect to each other along z axis are plotted by smaller and larger dots. Distance between nearest chains is a , distance between walls of nearest CNTs is d , CNT diameter is D , and the distance between centers of neighboring CNTs is $A=d+D$.

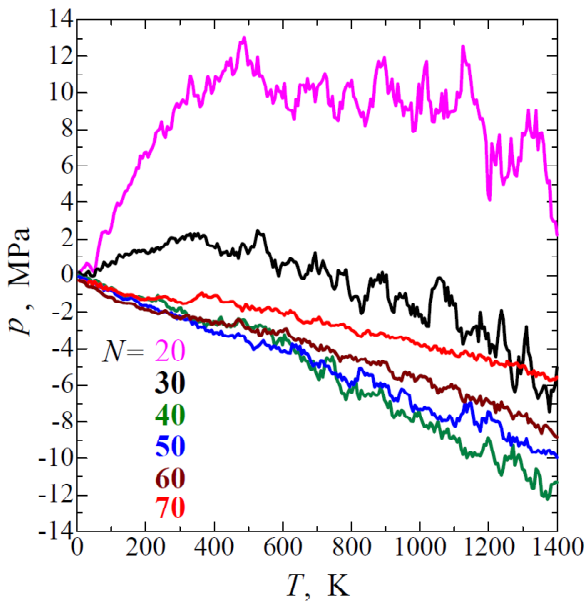


Fig. 2. Dependence of pressure on temperature for CNT bundles of different diameters.

for the case of $N=30$. Total number of atoms in the computational cell is $120N$.

The total energy of the system is described by the Hamiltonian, which includes four terms:

$$H = K + E_B + E_A + E_{vdW}. \quad (1)$$

Here K is the kinetic energy, E_B and E_A give the energy of valence bonds and valence angles, respectively. The E_{vdW} term describes the energy of van der Waals interactions. A detailed formulation of the model and description of the model parameters can be found in the

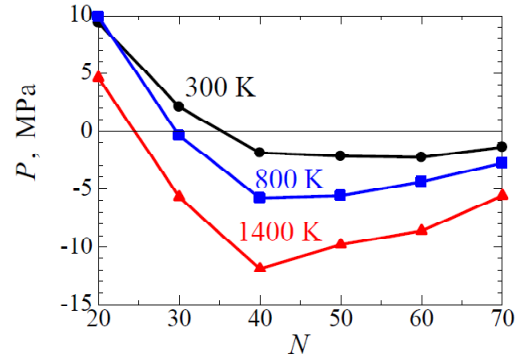


Fig. 3. Influence of CNT diameter on pressure at different temperatures: 300 K (circles), 800 K (squares), and 1400 K (triangles).

work [26]. The model has been successfully used to describe structure and peculiar mechanical properties of CNT bundles and other carbon 2D materials [27-31].

The Euler–Lagrange equations of motion can be derived from the Hamiltonian (1) using the Hamilton’s principle. The equations of motion are integrated with the use of the Störmer method of order six with the time step of 0.1 fs.

Simulation protocol is as follows. First, CNT bundle is relaxed at zero temperature and zero pressure. Then, using the NVT thermodynamic ensemble, the CNT bundle temperature linearly increased with time at a heating rate of 7 K/ps. A Langevin thermostat was used to control the temperature. The volume and size of the computational cell did not change during the simulation. The pressure was calculated as a function of temperature.

3. SIMULATION RESULTS

Fig. 2 shows the dependence of pressure $p = -(\sigma_{xx} + \sigma_{yy})/2$ on temperature for CNT bundles made of CNTs of various diameters. The CNT diameter is controlled by the number N of carbon atoms in the CNT cross section.

As seen in Fig. 2, for small temperatures, CNT bundles made of relatively small diameter CNTs ($N=20$ and 30) exhibit an increase in pressure with temperature at a constant volume, like most materials. However, at higher temperatures pressure starts to decrease and for $N=30$ becomes negative for $T > 800$ K. Bundles made of CNTs with $N=40$ and more, demonstrate pressure linearly decreasing with temperature. Negative pressure appears in heated bundles, which is rather unusual and requires an explanation. The rate of pressure decrease with temperature decreases with increasing N . Thus, maximal rate is demonstrated by the bundle made of CNTs with $N=40$ and at $T=1400$ K pressure drops down to about -12 MPa.

In Fig. 3, pressure as the function of CNT diameter, controlled by the number of carbon atoms in CNT cross section N is shown for three temperatures: 300 K (black



Fig. 4. Images of the structure of a CNT bundle at different temperatures: (a) 0 K, (b) 300 K, (c) 800 K and (d) 1400 K. The case of $N=30$ is presented.

circles), 800 K (blue squares), and 1400 K (red triangles). All three curves have a minimum. This means that for any temperature in the range under consideration, there is an optimal CNT diameter, which gives the most pronounced effect of negative pressure.

Snapshots of the CNT bundle structure at different temperatures can be seen in Fig. 4. The case of $N=30$ is presented. In (a), at zero temperature, CNT cross sections are close to circles. In (b), (c), and (d) the structures are presented at $T=300$, 800, and 1400 K, respectively. With increasing temperature, the cross sections of CNTs become more and more irregular.

4. CONCLUSIONS

The explanation of the anomalous effect manifested by a CNT bundle, namely, the appearance of negative pressure upon heating, is actually very simple. Recall that the covalent bonds in sp^2 carbon materials are very stiff compared to the valence bond angles. This is the reason for the very high tensile stiffness and low bending stiffness of the CNT wall. Thermal energy primarily excites low-energy vibrational modes, i.e., van der Waals modes, when CNTs vibrate as rigid bodies without in-

ternal deformations, and bending modes of the CNT walls. It is also clear that the walls of large-diameter CNTs are less rigid in bending than the walls of small-diameter CNTs. With this in mind, the results shown in Fig. 2 are easy to explain. For large CNT diameters ($N \gg 40$), thermal energy easily causes bending of the CNT walls, which, in turn, leads to an effective decrease in the CNT diameter. Shrinkage of CNT cross sections due to bending of their walls is the cause of negative pressure. A bundle of CNTs with $N=30$ at low temperatures ($T < 360$ K) shows an increase in pressure with temperature, but at higher temperatures the pressure begins to decrease and becomes negative for $T > 800$ K (see Fig. 2). The same tendency, but more pronounced, is observed for the CNT bundle in the case of $N=20$. This non-monotonic dependence of pressure on temperature can be explained if we take into account that small-diameter CNTs have a higher bending stiffness than large-diameter CNTs. Bending modes for small-diameter CNTs are excited at higher temperatures, which leads to an anomalous decrease in pressure with temperature. At low temperatures, the cross sections of small diameter CNTs vibrate like rigid rings with excitation of

van der Waals modes, and this leads to normal behavior when the pressure increases with temperature.

Our work can be concluded as follows. CNT bundles made of CNTs of a sufficiently large diameter demonstrate a negative coefficient of thermal expansion, which in our calculations at a constant volume leads to the appearance of negative pressure upon heating. This is due to the weak bending rigidity of the CNT walls. Thermal energy leads to bending of the CNT walls, which reduces their effective diameter and creates negative pressure.

ACKNOWLEDGEMENTS

This work was partly supported by the State Assignment of IMSPRAS, theme No. $\dot{R}\dot{R}\dot{R}\dot{R}-\dot{R}19-119021390108-5$. The simulation was partially carried out on a supercomputer of the RAS Supercomputer Center.

REFERENCES

- [1] V.A. Kuzkin and A.M. Krivtsov, *Nonlinear positive/negative thermal expansion and equations of state of a chain with longitudinal and transverse vibrations*, Phys. Status Solidi B, 2015, vol. 252, no. 7, pp. 1664-1670. <https://doi.org/10.1002/pssb.201451618>
- [2] X. Cheng, J. Yuan, X. Zhu, K. Yang, M. Liu and Z. Qi, *Origin of negative thermal expansion in Zn₂GeO₄ revealed by high pressure study*, J. Phys. D: Appl. Phys., 2018, vol. 51, no. 9, art. 095303. <https://doi.org/10.1088/1361-6463/aaa3d>
- [3] D.T. Ho, S.-Y. Kwon, H.S. Park and S.Y. Kim, *Negative Thermal Expansion of Ultrathin Metal Nanowires: A Computational Study*, Nano Lett., 2017, vol.17, no. 8, pp. 5113-5118. <https://doi.org/10.1021/acs.nanolett.7b02468>
- [4] M.T. Dove and H. Fang, *Negative thermal expansion and associated anomalous physical properties: review of the lattice dynamics theoretical foundation*, Rep. Prog. Phys., 2016. vol. 79, no. 6, art. 066503. <https://doi.org/10.1088/0034-4885/79/6/066503>
- [3????] K.W. Wojciechowski, F. Scarpa, J.N. Grima and A. Alderson, *Auxetics and other systems of negative characteristics*, Phys. Status Solidi B, 2015, vol. 252, no. 7, pp. 1421-1425. <https://doi.org/10.1002/pssb.201570348>
- [5] D.T. Ho, H.S. Park, S.Y. Kim and U. Schwingenschlög, *Graphene Origami with Highly Tunable Coefficient of Thermal Expansion*, ACS Nano, 2020, vol. 14, no. 7, pp. 8969-8974.
- [6] J. H. Belo, A. L. Pires, I. T. Gomes, V. Andrade, J. B. Sousa, R. L. Hadimani, D. C. Jiles, Y. Ren, X. Zhang, J. P. Araújo and A. M. Pereira, *Giant negative thermal expansion at the nanoscale in the multifunctional material Gd₅(Si,Ge)₄*, Phys. Rev. B, 2019, vol. 100, art. 134303. <https://doi.org/10.1103/PhysRevB.100.134303>
- [7] L. Forzani, C.A. Ramos, E. Vassallo Brigneti, A.M. Gennaro and R.R. Koropecski, *Negative thermal expansion of nanoporous anodic aluminum oxide membranes*, Appl. Phys. Lett., 2019, vol. 114, art. 111901. <https://doi.org/10.1063/1.5074083>
- [8] Q. Li, Zh. Deng, Y. Onuki, W. Wang, L. Li and Q. Sun, *In-plane low thermal expansion of NiTi via controlled cross rolling*, Acta Mater., 2021, vol. 204, art. 116506. <https://doi.org/10.1016/j.actamat.2020.116506>
- [9] J. Yuan, Y. Song, X. Xing and J. Chen, *Magnetic structure and uniaxial negative thermal expansion in antiferromagnetic CrSb*, Dalton Trans., 2020, vol. 49, pp. 17605-17611. <https://doi.org/10.1039/D0DT03277H>
- [10] Qilong Gao, Yu Sun, Naike Shi, Ruggero Milazzo, Simone Pollastri, Luca Olivi, Qingzhen Huang, Hui Liu, Andrea Sanson, Qiang Sun, Erjun Liang, Xianran Xing and Jun Chen., *Large isotropic negative thermal expansion in water-free Prussian blue analogues of ScCo(CN)₆*, Scripta Mater., 2020, vol. 187, pp. 119-124. <https://doi.org/10.1016/j.scriptamat.2020.05.041>
- [11] Martin T. Dove, Juan Du, Zhongsheng Wei, David A. Keen, Matthew G. Tucker and Anthony E. Phillips, *Quantitative understanding of negative thermal expansion in scandium trifluoride from neutron total scattering measurements*, Phys. Rev. B, 2020, vol. 102, art. 094105. <https://doi.org/10.1103/PhysRevB.102.094105>
- [12] Qilong Gao, Jiaqi Wang, Andrea Sanson, Qiang Sun, Erjun Liang, Xianran Xing and Jun Chen, *Discovering Large Isotropic Negative Thermal Expansion in Framework Compound AgB(CN)₄ via the Concept of Average Atomic Volume*, J. Am. Chem. Soc., 2020, vol. 142, no. 15, pp. 6935-6939. <https://doi.org/10.1021/jacs.0c02188>
- [13] L.R. Fokin, *Analysis of Data on Zero and Negative Thermal Expansion Coefficients of Materials*, High Temp., 2020, vol. 58, no. 2, pp. 173-183. <https://doi.org/10.1134/S0018151X20020054>
- [14] T. A. Bird, J. Woodland-Scott, L. Hu, M. T. Wharmby, J. Chen, A. L. Goodwin and M. S. Senn, *Anharmonicity and scissoring modes in the negative thermal expansion materials ScF₃ and CaZrF₆*, Phys. Rev. B, 2020, vol. 101, art. 064306. <https://doi.org/10.1103/PhysRevB.101.064306>

- [15] Chris Ablitt, Harriet McCay, Sarah Craddock, Lauren Cooper, Emily Reynolds, Arash A. Mostofi, Nicholas C. Bristowe, Claire A. Murray and Mark S. Senn, *Tolerance Factor Control of Uniaxial Negative Thermal Expansion in a Layered Perovskite*, Chem. Mater., 2020, vol. 32, no. 1, pp. 605-610. <https://doi.org/10.1021/acs.chemmater.9b04512>
- [16] Yuzhu Song, Qiang Sun, Meng Xu, Ji Zhang, Yiqing Hao, Yongqiang Qiao, Shantao Zhang, Qingzhen Huang, Xianran Xing and Jun Chen, *Negative thermal expansion in (Sc,Ti)Fe₂ induced by an unconventional magnetovolume effect*, Mater. Horizons, 2020, vol. 7, pp. 275-281. <https://doi.org/10.1039/C9MH01025D>
- [17] D. Bocharov, M. Krack, Y. Rafalskij, A. Kuzmin and J. Purans, *Ab initio molecular dynamics simulations of negative thermal expansion in ScF₃: The effect of the supercell size*, Comp. Mater. Sci., 2020, vol. 171, art. 109198. <https://doi.org/10.1016/j.commatsci.2019.109198>
- [18] Y. Oba, T. Tadano, R. Akashi and S. Tsuneyuki, *First-principles study of phonon anharmonicity and negative thermal expansion in ScF₃*, Phys. Rev. Mater., 2019, vol. 3, art. 033601. <https://doi.org/10.1103/PhysRevMaterials.3.033601>
- [19] N.C. Burch, S.J. Baxter, J. Heinen, A. Bird, A. Schneemann, D. Dubbeldam and A.P. Wilkinson, *Negative thermal expansion design strategies in a diverse series of metal-organic frameworks*, Adv. Funct. Mater., 2019, vol. 29, no. 48, art. 1904669. <https://doi.org/10.1002/adfm.201904669>
- [20] Ch. Schneider, D. Bodesheim, M. G. Ehrenreich, V. Crocellà, J. Mink, R. A. Fischer, Keith T. Butler and G. Kieslich, *Tuning the Negative Thermal Expansion Behavior of the Metal-Organic Framework Cu₃BTC₂ by Retrofitting*, J. Am. Chem. Soc., 2019, vol. 141, no. 26, pp. 10504-10509. <https://doi.org/10.1021/jacs.9b04755>
- [21] C.S. Coates and A.L. Goodwin, *How to quantify isotropic negative thermal expansion: magnitude, range, or both?*, Mater. Horizons, 2019, vol. 6, pp. 211-218. <https://doi.org/10.1039/C8MH01065J>
- [22] Stella d'Ambrumenil, Mohamed Zbiri, Ann M. Chippindale, Simon J. Hibble, Elena Marelli and Alex C. Hannon, *Lattice dynamics and negative thermal expansion in the framework compound ZnNi(CN)₄ with two-dimensional and three-dimensional local environments*, Phys. Rev. B, 2019, vol. 99, art. 024309. <https://doi.org/10.1103/PhysRevB.99.024309>
- [23] A. Sanson, *On the switching between negative and positive thermal expansion in framework materials*, Mater. Res. Lett., 2019, vol. 7, pp. 412-417. <https://doi.org/10.1080/21663831.2019.1621957>
- [24] T.-C. Lim, *Negative Environmental Expansion for Interconnected Array of Rings and Sliding Rods*, Phys. Status Solidi B, 2019, vol. 256, no. 1, art. 1800032. <https://doi.org/10.1002/pssb.201800032>
- [25] Naike Shi, Qilong Gao, Andrea Sanson, Qiang Li, Longlong Fan, Yang Ren, Luca Olivi, Jun Chen and Xianran Xing, *Negative thermal expansion in cubic FeFe(CN)₆ Prussian blue analogues*, Dalton Trans., 2019, vol. 48, pp. 3658-3663. <https://doi.org/10.1039/C8DT05111A>
- [26] D.U. Abdullina, E.A. Korznikova, V.I. Dubinko, D.V. Laptev, A.A. Kudreyko, E.G. Soboleva, S.V. Dmitriev and K. Zhou, *Mechanical Response of Carbon Nanotube Bundle to Lateral Compression*, Computation, 2020, vol. 8, no. 2 (2020), art. 27. <https://doi.org/10.3390/computation8020027>
- [27] L.Kh. Rysaeva, R.T. Murzaev, A.A. Kudreyko, E.A. Korznikova and S.V. Dmitriev, *Behaviour of carbon nanotube bundle under quasistatic and dynamic transverse compression*, IOP Conf. Ser.: Mater. Sci. Eng., 2020, vol. 1008, art. 012063. <https://doi.org/10.1088/1757-899X/1008/1/012063>
- [28] L.K. Rysaeva, D.V. Bachurin, R.T. Murzaev, D.U. Abdullina, E.A. Korznikova, R.R. Mulyukov and S.V. Dmitriev, *Evolution of the Carbon Nanotube Bundle Structure under Biaxial and Shear Strains*, Facta Universitatis, Series: Mechanical Engineering, 2020, vol. 18, no. 4, pp. 525-536. <https://doi.org/10.22190/FUME201005043R>
- [29] L.K. Rysaeva, E.A. Korznikova, R.T. Murzaev, D.U. Abdullina, A.A. Kudreyko, J.A. Baimova, D.S. Lisovenko and S.V. Dmitriev, *Elastic damper based on the carbon nanotube bundle*, Facta Universitatis-Series Mechanical Engineering, Facta Universitatis, Series: Mechanical Engineering, 2020, vol. 18, no. 1, pp. 1-12. <https://doi.org/10.22190/FUME200128011R>
- [30] E.A. Korznikova, L.K. Rysaeva, A.V. Savin, E.G. Soboleva, E.G. Ekomasov, M.A. Ilgamov and S.V. Dmitriev, *Chain Model for Carbon Nanotube Bundle under Plane Strain Conditions*, Materials, 2019, vol. 12, no. 23, art. 3951. <https://doi.org/10.3390/ma12233951>
- [31] A.V. Savin, E.A. Korznikova, S.V. Dmitriev and E.G. Soboleva, *Graphene nanoribbon winding around carbon nanotube*, Comp. Mater. Sci., 2017, vol. 135, pp. 99-108. <https://doi.org/10.1016/j.commatsci.2017.03.047>